From gravitational action to small-scale galaxy correlation functions

arXiv: 2110.00328, 2110.00566, 2110.10033

Cheng-Zong Ruan

cheng-zong.ruan@durham.ac.uk

Friday Lunchtime Astrophysics Talks, October 29, 2021

Overview - from gravitational action to correlation functions

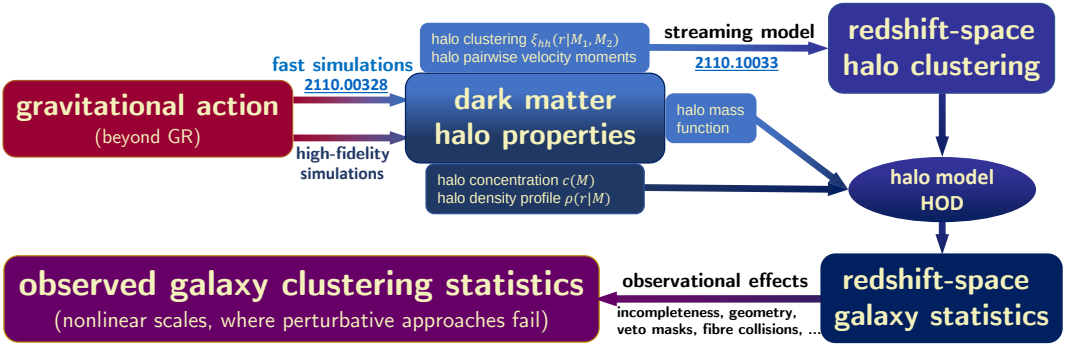

Modified Gravity (MG) N-body Simulations

a viable MG theory:

- solar system tests (needless to say);
- from the neutron star binary GW170817 and its electromagnetic counterpart GRB170817A: for $z \lesssim 0.1$, speed of light is c;
- from BBN and CMB: gives the correct linear perturbation predictions;
- from BAO: a weak gaussian prior on $H(z)$ at redshifts corresponding to the existing angular-diameter distance measurements from BAO;
- from ghost and gradient instabilities for the perturbation modes (checked by theorists).

Full vs Phenomenological MG Modeling

Chapman et al. 2021, 2106.14961,
eBOSS LRG emulator-based analysis

density and theory of gravity. Our parameter γ_f is defined as $f/f_{\Lambda\mathrm{CDM}}$, and all halo velocities are rescaled by this value.[8]

5.1 Headline results

We fit the eBOSS LRG monopole, quadrupole, and projected correlation function over scales $0.1 < r < 60\,h^{-1}$Mpc using /a MCMC sampler. We restrict the cosmological parameter ig the AEMULUS training prior described in Sec. 3.7, but do not include any external data. We obtain a value of $\gamma_f = 0.767 \pm 0.052$, 4.5σ below what would be expected in a ΛCDM+GR universe. The 1D and 2D likelihood contours of the full parameter set are shown in Fig. 16. All well constrained parameters are within the prior ranges described in Table 1, and the parameters that are most impactful of the same sample. Using the full separation range of our measurement we find a 4.5σ tension in the amplitude of the halo velocity field with the expectation for a ΛCDM universe. This tension is driven by the non-linear scales of our analysis and so may not be well modelled by a change in the linear growth rate, but may instead reflect a breakdown in the HOD model used in the emulator.

- phenomenological parameterisation:

$$\boldsymbol{v} \xrightarrow{\text{rescale}} \gamma_f\, \boldsymbol{v}_{\mathrm{GR}}\,, \qquad \gamma_f^{\text{best-fit}} \sim 1?$$

- big news: $\gamma_f \neq 1$ with 4.5σ confidence level?!
- sysmatics difficult to control
- based on some simplified assumptions

Modified Gravity (MG) N-body Simulations

- Einstein-Hilbert action $\xrightarrow{\text{variation w.r.t. inverse of metric}}$ Einstein field equation
- two types of actions beyond E-H are considered in MG-GLAM:
  - conformal coupling models:

$$S = \int \mathrm{d}^4x\sqrt{-g}\Big[\underbrace{\frac{M_{\rm Pl}^2}{2}R}_{\text{E-H}}\underbrace{-\frac{1}{2}\nabla^\mu\phi\nabla_\mu\phi - V(\phi)}_{\text{conformal coupling terms}}\Big] + \int \mathrm{d}^4x\sqrt{-\hat{g}}\,\mathcal{L}^{\rm m}[\psi_i, \hat{g}_{\mu\nu}]$$

  - derivative coupling models:

$$S = \int \mathrm{d}^4x\sqrt{-g}\Big[\underbrace{\frac{M_{\rm Pl}^2}{2}R}_{\text{E-H}} + \underbrace{K\Big[(\nabla\phi)^2, (\nabla^2\phi)\Big] - V(\phi)}_{\text{derivative coupling terms}}\Big] + \int \mathrm{d}^4x\sqrt{-\hat{g}}\,\mathcal{L}^{\rm m}[\psi_i, \hat{g}_{\mu\nu}]$$

Modified Gravity (MG) N-body Simulations

- conformal coupling models: $(\hat{g}_{\mu\nu} = A^2(\phi) g_{\mu\nu})$

$$S = \int \mathrm{d}^4x\sqrt{-g}\Big[\frac{M_{\rm Pl}^2}{2}R - \frac{1}{2}\nabla^\mu\phi\nabla_\mu\phi - V(\phi)\Big] + \int \mathrm{d}^4x\sqrt{-\hat{g}}\,\mathcal{L}^{\rm m}[\psi_i, \hat{g}_{\mu\nu}],$$

- coupled quintessence: $A(\phi) = e^{\beta\phi/M_{\rm Pl}}$, $V(\phi) = \dfrac{\Lambda^4 M_{\rm Pl}^\alpha}{\phi^\alpha}$
- symmetron: $A(\phi) = 1 + \dfrac{\phi^2}{2M^2}$, $V(\phi) = V_0 - \dfrac{1}{2}\mu^2\phi^2 + \dfrac{1}{4}\zeta\phi^4$
- $f(R)$ gravity:

$$S = \int \mathrm{d}^4x\sqrt{-g}\Big[\frac{M_{\rm Pl}^2}{2}R + f(R)\Big] + \int \mathrm{d}^4x\sqrt{-\hat{g}}\,\mathcal{L}^{\rm m}[\psi_i, \hat{g}_{\mu\nu}],$$

N-body simulations - $f(R)$ gravity

- $$\begin{cases} \dfrac{\mathrm{d}\boldsymbol{x}}{\mathrm{d}a} = \dfrac{\boldsymbol{p}}{a^3 H}, \qquad \dfrac{\mathrm{d}\boldsymbol{p}}{\mathrm{d}a} = -\dfrac{\nabla\Phi}{aH} \\ \nabla^2\Phi = 4\pi G a^2(\delta\rho_m) - \dfrac{c^2}{2}\nabla^2 f_R \\ \nabla^2 f_R = \dfrac{a^2}{3c^2}[\delta R - 8\pi G(\delta\rho_m)] \end{cases}$$

$$\begin{cases} \text{GR part (density field, Newtonian potential,} \\ \text{time integration), implemented in GLAM} \\ \text{MG part: extra scalar field } f_R(\boldsymbol{x}, a) \end{cases}$$

GLAM and MG-GLAM

• GLAM (Anatoly Klypin and Francisco Prada, arXiv:1701.05690): vanilla Particle-Mesh (PM) N-body code for the massive production of galaxy survey mocks
• efficiently implemented FFT Poisson solver
• pure PM code (resolution fixed), no tree-PM (e.g. GADGET, AREPO) or Adaptive-Mesh-Refinement algorithms (e.g. RAMSES); sacrificing small-scale accuracy for speed

• parallelisation with OPENMP directives (MPI is used only to run many realisations): one job, one computational node

```
for fR0 in ...: for Omegam in ...: for H0 in ...:
    sbatch MG-GLAM-job(fR0, Omegam, H0, ...)   #SBATCH --ntasks 1
```

N-body codes

Name	Type	Resolution Mpch	Halos Subhalos	Steps
FastPM	PM	0.20	No No	40
COLA	PM	0.3	No No	40
GLAM	PM	0.1-0.3	Yes No	140-180
Abacus	P3M	0.06-0.1	Yes No	
GADGET GreeM	TreePM	0.003-0.001	Yes Yes	5000

Table 2. Rescaled CPU and memory required by different PM codes to make one 150 time-steps simulation with 1 billion particles and $N_g = 3000$ mesh.

	GLAM	COLA[1]	ICE-COLA[2]	FastPM[3]
CPU, hrs	146	220	320	567
Memory, Gb	123	240	325	280

[1]Koda et al. (2016), [2]Izard et al. (2015), [3]Feng et al. (2016)

credit: Anatoly Klypin

MG-GLAM code tests:

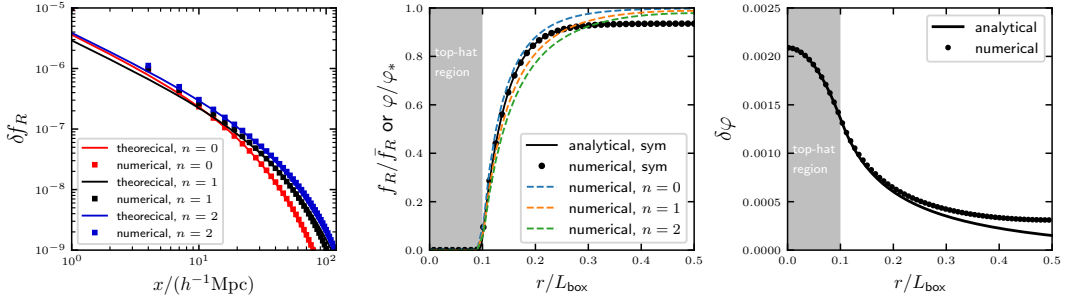

density configurations with high symmetry (e.g. point mass, top-hat density)

comparison with high-fidelity simulation codes MG-GADGET and MG-AREPO

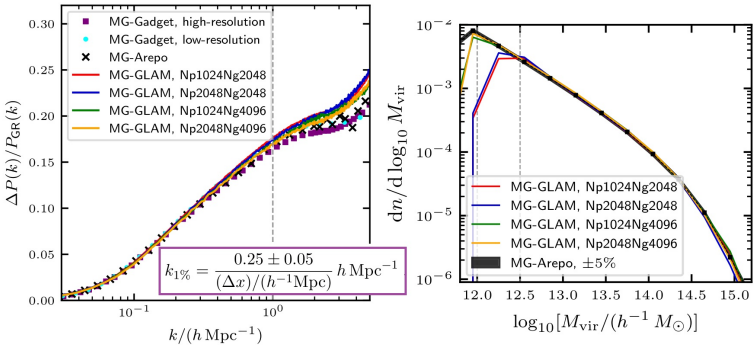

MG-GLAM simulations: $L = 1024\,h^{-1}{\rm Mpc}$, 2048^3 particles, 4096^3 grids, $k_{1\%} = 1\,h\,{\rm Mpc}^{-1}$, ~ 30 h for a $f(R)$ gravity simulation with 128 threads using one node of the SKUN6@IAA-CSIC supercomputer, 100-300 times faster than ECOSMOG and MG-AREPO

GLAM and MG-GLAM

$$S = \frac{M_{\rm Pl}^2}{2}\int \mathrm{d}^4x\sqrt{-g}\,[R + f(R)]$$

gravitational action
(beyond GR)

MG-GLAM
2110.00328

dark matter halo properties

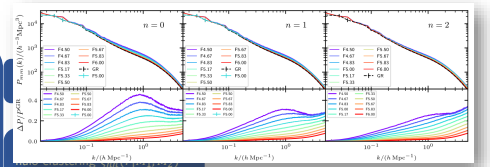

halo concentration $c(M)$
halo density profile $\rho(r|M)$

$$\underbrace{\{\Omega_m, \Omega_b, h, \sigma_8, \cdots\}}_{\text{cosmological}} \times \underbrace{\{M_{\rm sat}, M_{\rm cut}, \alpha, \sigma_{\log M}, \cdots\}}_{\text{HOD}} \times \underbrace{\{f_{R0}, n, \cdots\}}_{\text{MG}} \times \underbrace{\left\{\sum m_\nu\right\}}_{\text{neutrinos}}$$

Galaxy Clustering

- small-scale galaxy redshift-space correlation function multipole moments:

$$\xi^{\rm S}_{0,2,4}\Big(s \lesssim 20\,h^{-1}{\rm Mpc};\ \underbrace{\Omega_{m0}, H_0, \cdots}_{\text{cosmological}};\ \underbrace{\bar{f}_{R0}, \cdots}_{\text{MG}};\ \underbrace{M_{\rm cut}, M_{\rm sat}, \alpha, \cdots}_{\text{HOD}}\Big)$$

- small-scale: perturbation theory based models fail, needs simulation-based emulator [existing simulation suite: FORGE (Christian Arnold, Baojiu Li et al., arXiv:2109.04984)]
- galaxy bias model: halo model and Halo Occupation Distribution (HOD) [in progress]
- real-to-redshift space mapping: the streaming model of redshift space distortions (RSD) and the Skew-T (Carolina Cuesta-Lazaro et al., 2020, arXiv:2002.02683) pairwise velocity distribution [done. arXiv:2110.10033]

Real-to-Redshift Space Mapping

The streaming model of RSD (Scoccimarro 2004) provides the exact relationship between real- and redshift-space correlation functions:

$$1+\xi^{\rm S}(s_\perp, s_\parallel) = \int_{-\infty}^{\infty} {\rm d}r_\parallel \left[1+\xi^{\rm R}(r)\right] \mathcal{P}(s_\parallel - r_\parallel | \boldsymbol{r})$$

- halo real-space correlation functions
- halo pairwise velocity moments

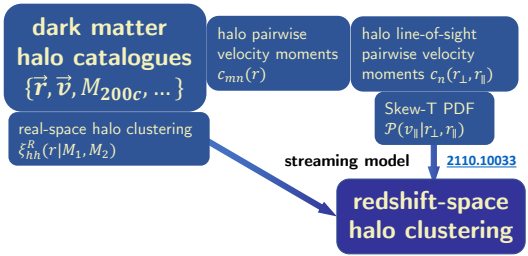

Real-to-Redshift Space Mapping

- halo line-of-sight pairwise velocity PDF $\mathcal{P}(v_\parallel|r_\perp, r_\parallel)$, moments of PDF:

$$m_n(\boldsymbol{r}) = \int \mathrm{d}v_\parallel \, (v_\parallel)^n \mathcal{P}(v_\parallel|\boldsymbol{r})$$

$$c_n(\boldsymbol{r}) = \int \mathrm{d}v_\parallel \, \big[v_\parallel - m_1(\boldsymbol{r})\big]^n \mathcal{P}(v_\parallel|\boldsymbol{r})$$

- Gaussian:

$$\mathcal{P}_\mathrm{G}(v_\parallel|\boldsymbol{r}) = \frac{1}{\sqrt{2\pi c_2(\boldsymbol{r})}} \exp\left[-\frac{\big(v_\parallel - m_1(\boldsymbol{r})\big)^2}{2c_2(\boldsymbol{r})}\right]$$

- Skew-T:

$$\mathcal{P}_\mathrm{ST}\big(v_\parallel; v_c(r), w(r), \alpha(r), \nu(r)|\boldsymbol{r}\big) = \frac{2}{w} t_1(v_\parallel - v_c|1, \nu)$$
$$\times T_1\left(\alpha \frac{v_\parallel - v_c}{w}\left[\frac{\nu+1}{\nu + \big((v_\parallel - v_c)/w\big)^2}\right]^{1/2}; \nu+1\right)$$

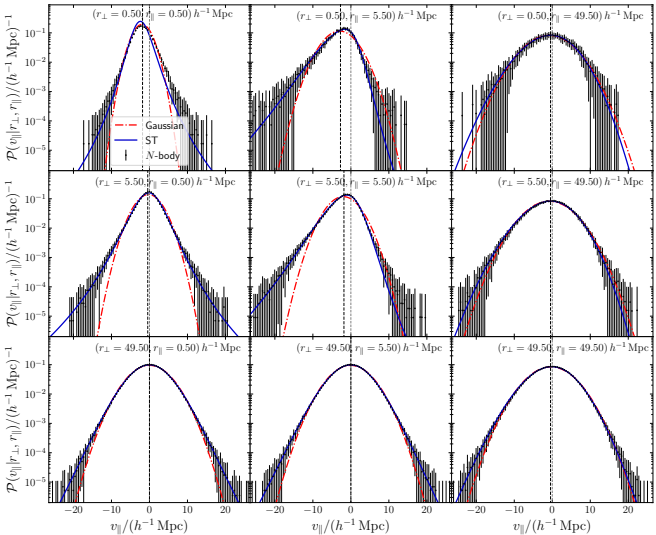

Real-to-Redshift Space Mapping

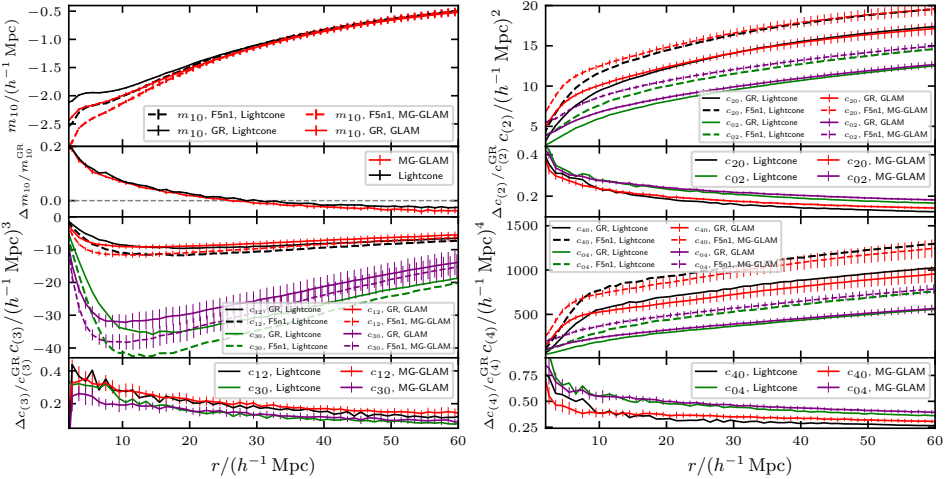

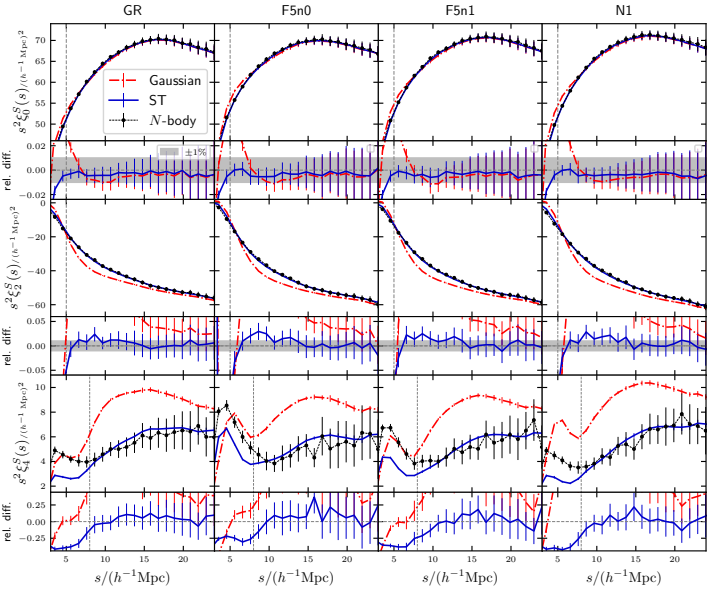

monopole: $\gtrsim 2\,h^{-1}\,\mathrm{Mpc}$
quadrupole: $\gtrsim 5\,h^{-1}\,\mathrm{Mpc}$
hexadecapole: $\gtrsim 8\,h^{-1}\,\mathrm{Mpc}$

the streaming model predictions (blue lines) are less noisy than the simulation measurements (black dots)

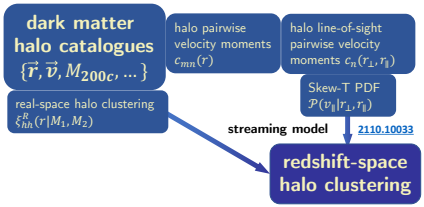

Cosmological Emulator

perturbation theory-based methods fail at small, highly non-linear scales:

- the combined Gaussian Streaming Model (GSM) and Convolutional Lagrangian Perturbation Theory (CLPT)
- TNS model: the perturbative expansion of the steaming model expressions
- effective field theory approaches

Bautista et al. 2020,
eBOSS, LRG, configuration-space
arXiv: 2007.08993

Overall, these tests performed on the NSERIES mocks allow us to define the optimal fitting ranges of scales for both RSD models. Minimizing the bias of the models while keeping $r_{\rm min}$ as small as possible, we eventually adopt the following optimal ranges:

- TNS model: $20 < r < 130h^{-1}$Mpc for ξ_0 and ξ_2, and $25 < r < 130h^{-1}$Mpc for ξ_4
- CLPT-GS model: $25 < r < 130h^{-1}$Mpc for all multipoles,

which serve as baseline in the following. We compare the performance of the two models using these ranges in the following sections.

Cosmological Emulator

simulation-based emulator needs:

- an efficient parameter sampling strategy
- an effective interpolation scheme

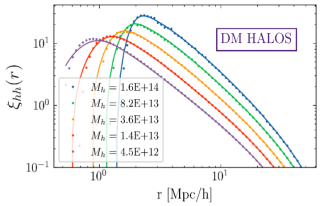

$\xi_{hh} = \phi(cosmology, M_h, r, z)$

credit: Carolina Cuesta-Lazaro

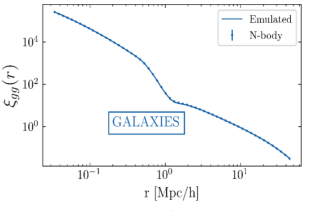

$\xi_{gg} \rightarrow \int dM_h\ \xi_{hh}$

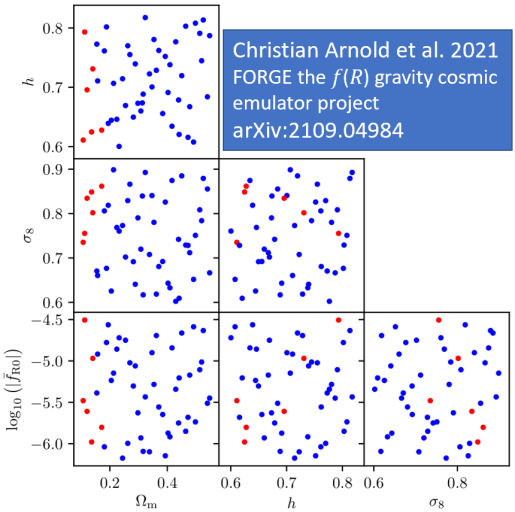

Christian Arnold et al. 2021
FORGE the $f(R)$ gravity cosmic emulator project
arXiv:2109.04984

Halo Model and HOD

$$\xi^S_{gg}(\boldsymbol{s}) = \xi^S_{gg,1h}(\boldsymbol{s}) + \xi^S_{gg,2h}(\boldsymbol{s})$$ 1-halo and 2-halo terms

$$\xi^S_{gg,2h}(\boldsymbol{s}) = \xi^S_{cc}(\boldsymbol{s}) + \xi^S_{cs}(\boldsymbol{s}) + \xi^S_{sc}(\boldsymbol{s}) + \xi^S_{ss}(\boldsymbol{s})$$ HOD: central and satellite galaxy separation

$$\xi^S_{cc}(\boldsymbol{s}) = \frac{1}{\bar{n}_g^2}\int dM_1 \int dM_2 \frac{dn}{dM}(M_1)\frac{dn}{dM}(M_2)\langle N_c\rangle(M_1)\langle N_c\rangle(M_2)\xi^S_{hh}(\boldsymbol{s}|M_1, M_2)$$

$$\xi^S_{cs}(\boldsymbol{s}) = \frac{1}{\bar{n}_g^2}\int dM_1 \int dM_2 \frac{dn}{dM}(M_1)\frac{dn}{dM}(M_2)\langle N_c\rangle(M_1)\langle N_s\rangle(M_2) \int d\boldsymbol{s}'\rho^s(\boldsymbol{s}'|M_2)\xi^S_{hh}(\boldsymbol{s}-\boldsymbol{s}'|M_1, M_2)$$

$$\xi^S_{sc}(\boldsymbol{s}) = \frac{1}{\bar{n}_g^2}\int dM_1 \int dM_2 \frac{dn}{dM}(M_1)\frac{dn}{dM}(M_2)\langle N_c\rangle(M_2)\langle N_s\rangle(M_1) \int d\boldsymbol{s}'\rho^s(\boldsymbol{s}'|M_1)\xi^S_{hh}(\boldsymbol{s}-\boldsymbol{s}'|M_1, M_2)$$

$$\xi^S_{ss}(\boldsymbol{s}) = \frac{1}{\bar{n}_g^2}\int dM_1 \int dM_2 \frac{dn}{dM}(M_1)\frac{dn}{dM}(M_2)\langle N_s\rangle(M_2)\langle N_s\rangle(M_1) \int d\boldsymbol{s}''\rho^s(\boldsymbol{s}''|M_2)\int d\boldsymbol{s}'\rho^s(\boldsymbol{s}'|M_1)\xi^S_{hh}(\boldsymbol{s}-\boldsymbol{s}''-\boldsymbol{s}'|M_1, M_2)$$

ingredients:

halo mass function

the mean HOD for central and satellite galaxies

halo redshift-space 2-pt correlation functions

halo density profile

credit:
Carolina Cuesta-Lazaro

Overview - from gravitational action to correlation functions